

Density Evolution for Deterministic Generalized Product Codes with Higher-Order Modulation

Christian Häger[†], Alexandre Graell i Amat[†], Henry D. Pfister[‡], and Fredrik Brännström[†]

[†]Department of Signals and Systems, Chalmers University of Technology, Gothenburg, Sweden

[‡]Department of Electrical and Computer Engineering, Duke University, Durham, North Carolina

Abstract—Generalized product codes (GPCs) are extensions of product codes (PCs) where coded bits are protected by two component codes but not necessarily arranged in a rectangular array. It has recently been shown that there exists a large class of deterministic GPCs (including, e.g., irregular PCs, half-product codes, staircase codes, and certain braided codes) for which the asymptotic performance under iterative bounded-distance decoding over the binary erasure channel (BEC) can be rigorously characterized in terms of a density evolution analysis. In this paper, the analysis is extended to the case where transmission takes place over parallel BECs with different erasure probabilities. We use this model to predict the code performance in a coded modulation setup with higher-order signal constellations. We also discuss the design of the bit mapper that determines the allocation of the coded bits to the modulation bits of the signal constellation.

I. INTRODUCTION

A product code (PC) is defined as the set of all rectangular arrays such that each row and column is a codeword in some linear component code [1]. Assuming efficient iterative decoding of the component codes (e.g., algebraic bounded-distance decoding (BDD) of Bose–Chaudhuri–Hocquenghem (BCH) codes), PCs are an excellent choice for error-correcting codes in high-speed applications such as fiber-optical communications [2]. Indeed, PCs are standardized in [3] and several extensions of PCs, e.g., staircase [4] and braided codes [5], have been proposed for such systems. We refer to these codes as generalized product codes (GPCs).

Motivated by the recent trend towards spectrally-efficient fiber-optical systems [6], our objective in this paper is to characterize the asymptotic performance of GPCs under iterative BDD in a coded modulation scenario. Similar to [7], we consider pragmatic bit-interleaved coded modulation (BICM) with a hard-decision symbol detector. This setup can be modeled as a set of parallel binary symmetric channels (BSCs). The hard-decision detector comes at the price of a performance loss compared to calculating “soft” reliability information about the coded bits. However, it is also significantly less complex and therefore an attractive candidate for high-speed systems.

In [8], the authors propose a deterministic (i.e., non-ensemble-based) construction for GPCs and study the asymptotic performance over the binary erasure channel (BEC) under

iterative BDD in the form of a density evolution (DE) analysis. In this paper, the main contribution is to extend this analysis to the case where transmission takes place over parallel BECs with different erasure probabilities. Ignoring miscorrections in the BDD, the analysis applies without change also to parallel BSCs. The derived DE analysis can then be used to predict the waterfall performance of the GPCs for the considered BICM system.

As an application, we consider the problem of optimizing the bit mapper (or interleaver) that determines the allocation of the coded bits from the GPC to the modulation bits of the signal constellation. This problem has been studied in detail for low-density parity-check codes (see, e.g., [9] and references therein for an overview in the context of fiber-optical communications). Here, we show that by taking advantage of the unequal error protection offered by a higher-order signal constellation, the performance of deterministic GPCs can be improved at almost no increased system complexity.

Notation. We use boldface letters for vectors and matrices (e.g., \mathbf{x} and \mathbf{A}), and denote the transpose by $(\cdot)^T$. The symbols $\mathbf{0}$ and $\mathbf{1}$ denote the all-zero and all-one vectors, where the length is apparent from the context. For vectors, we use $\mathbf{x} \succeq \mathbf{y}$ if $x_i \geq y_i$ for all i . We also define $[m] \triangleq \{1, 2, \dots, m\}$.

II. DETERMINISTIC GENERALIZED PRODUCT CODES

In this section, we review the parametrized family of GPCs proposed in [8]. A GPC in this family is denoted by $\mathcal{C}_n(\boldsymbol{\eta}, \boldsymbol{\tau})$, where n corresponds to the total number of constraint nodes (CNs) in the underlying Tanner graph and $\boldsymbol{\eta}$ is a binary symmetric $L \times L$ matrix that defines the graph connectivity. The parameter $\boldsymbol{\tau}$ is used to specify GPCs that employ component codes with different erasure-correcting capabilities and is described in Section II-A below.

To construct the Tanner graph that defines $\mathcal{C}_n(\boldsymbol{\eta}, \boldsymbol{\tau})$, assume that there are L positions. Then,

- 1) place $d \triangleq n/L$ CNs at each position and
- 2) connect each CN at position i to each CN at position j through a variable node (VN) if and only if $\eta_{i,j} = 1$.

For given n and $\boldsymbol{\eta}$, this construction fully specifies the degrees of all CNs, i.e., the lengths of all component codes. In particular, CNs at position i have degree $d \sum_{j \neq i} \eta_{i,j} + \eta_{i,i}(d-1)$, where the second term arises from the convention that we cannot connect a CN to itself if $\eta_{i,i} = 1$.

While our code construction is given in terms of a Tanner graph, GPCs have a natural array representation which we

This work was partially funded by the Swedish Research Council under grant #2011-5961. The work of H. Pfister was supported in part by the National Science Foundation (NSF) under Grant No. 1320924. Any opinions, findings, conclusions, and recommendations expressed in this material are those of the authors and do not necessarily reflect the views of the NSF.

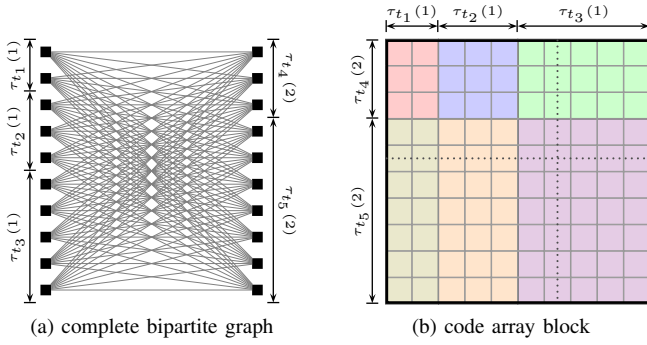


Fig. 1. Illustrations corresponding to off-diagonal entries in η , i.e., $\eta_{i,j} = 1$ for $i \neq j$. The distributions specifying the erasure-correcting capabilities are $\tau_{t_1}(1) = 0.2$, $\tau_{t_2}(1) = 0.3$, $\tau_{t_3}(1) = 0.5$, $\tau_{t_4}(2) = 0.3$, and $\tau_{t_5}(2) = 0.7$.

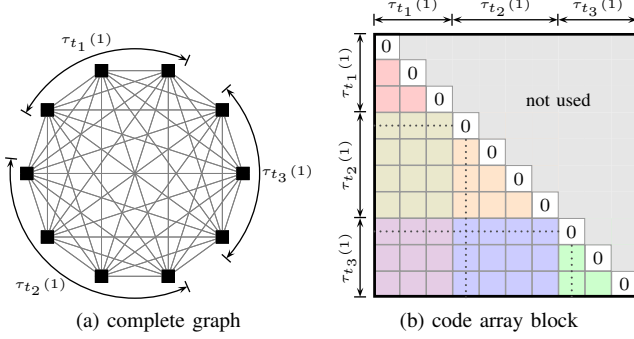


Fig. 2. Illustrations corresponding to diagonal entries in η , i.e., $\eta_{i,i} = 1$. The distribution specifying the erasure-correcting capabilities is assumed to be $\tau_{t_1}(1) = 0.3$, $\tau_{t_2}(1) = 0.4$, and $\tau_{t_3}(1) = 0.3$.

review in the following. In general, the code array of $\mathcal{C}_n(\eta, \tau)$ consist of *blocks*, where d is referred to as the block size.

Example 1. A PC is obtained for $L = 2$ and $\eta = \begin{pmatrix} 0 & 1 \\ 1 & 0 \end{pmatrix}$. Fig. 1(a) shows the simplified Tanner graph for $n = 20$ (i.e., $d = 10$), where VNs are represented by edges. The graph corresponds to a complete bipartite graph. The CNs at the two positions correspond to “row codes” and “column codes”, respectively. The $d \times d$ code array is shown in Fig. 1(b), where colors and arrows can be ignored for now. One particular row/column constraint is indicated by the dotted lines. \triangle

In general, an off-diagonal entry in the lower triangular part of η (i.e., connecting CNs at two different positions) gives rise to d^2 VNs and a square code array block as shown in Fig. 1(b). On the other hand, a diagonal entry in η (i.e., connecting CNs at the same position) only gives rise to $\binom{d}{2}$ VNs.

Example 2. Consider the case where $L = 1$ and $\eta = 1$. Fig. 2(a) shows the simplified Tanner graph corresponding to a complete graph for $n = 10$ (i.e., $d = 10$). The code is referred to as a half-product code (HPC) [10], [11]. Each VN (i.e., each edge in the simplified Tanner graph) can be associated with an entry in the lower (or upper) triangular part of the code array block, as shown in Fig. 2(b). Component code constraints act on L-shapes in the array, i.e., partial rows and columns, which include a frozen 0-bit on the array diagonal. Two different code constraints are visualized in Fig. 2(b) by the dotted lines. \triangle

The graphs and arrays in Figs. 1 and 2 are the fundamental building blocks in the code construction. Examples of GPCs consisting of multiple blocks include staircase [4] and half-

braided codes [11], [12], which can both be seen as special cases in our construction (see [13] for details). The number of VNs—and therefore the length of $\mathcal{C}_n(\eta, \tau)$ —is obtained by counting the bits in all code array blocks according to $m = \binom{d}{2} \sum_{i=1}^L \eta_{i,i} + d^2 \sum_{1 \leq i < j \leq L} \eta_{i,j}$.

A. Erasure-Correcting Capabilities and VN Classes

So far, we have only specified the lengths of the component codes associated with the CNs. As a last step, we assign different erasure-correcting capabilities to the component codes. To that end, for each $i \in [L]$, let $\tau(i) = (\tau_1(i), \dots, \tau_{t_{\max}}(i))^T$ be a probability vector of length t_{\max} (i.e., $\mathbf{1}^T \tau(i) = 1$ and $\tau(i) \succeq \mathbf{0}$), where $\tau_t(i)$ denotes the fraction of component codes at position i which can correct t erasures and t_{\max} is the maximum erasure-correcting capability. Erasure-correcting capabilities are assigned in a consecutive fashion as indicated by the arrows in Figs. 1 and 2. The collection of all probability vectors (or distributions) is denoted by $\tau = (\tau(i))_{i=1}^L$.

The class of a CN and the corresponding component code is given by the pair (i, t) , where i refers to the position in the Tanner graph and t to the erasure-correcting capability. The code construction is given in terms of CN classes. This is somewhat counterintuitive since typically coded bits are more tangible than code constraints. Therefore, a description in terms of VN classes may be preferable. However, VN classes are secondary in our construction: The class of a VN depends on the classes of the *two* CNs that it is connected to. In particular, a VN class is defined by two parameter pairs (i, t) and (j, t') , i.e., four parameters in total. The total number of VN classes is denoted by K . We assume some fixed and arbitrary indexing of the VN classes. The number of bits in the k -th VN class is denoted by m_k for $k \in [K]$.

VN classes will become important in the next section, where we discuss how the different coded bits are transmitted over parallel channels. Roughly speaking, the VN class determines the protection level of the corresponding bit. The protection level depends on the block that the bit belongs to (i.e., the pair (i, j)) and the strengths of the two associated component codes (i.e., the pair (t, t')). Observe that employing component codes with different erasure-correcting capabilities essentially subdivides each code array block into subblocks. This is illustrated in Figs. 1 and 2, where arrows indicate groups of component codes with the same erasure-correcting capability and colors represent different VN classes. Note that we have $K = 6$ in both cases.

III. CHANNEL MODEL AND BIT MAPPER

We assume that a codeword of $\mathcal{C}_n(\eta, \tau)$ is transmitted over a set of M parallel independent BECs with different erasure probabilities p_1, \dots, p_M . The allocation of the coded bits to the BECs is determined by a bit mapper. In particular, let $\mathbf{A} = [a_{k,q}]$ be the bit mapper matrix of size $K \times M$, where $a_{k,q}$ denotes the fraction of coded bits from the k -th VN class (out of m_k total bits) that are allocated to the q -th BEC. A valid bit mapper matrix is such that each row in \mathbf{A} is a probability

vector (i.e., for each $k \in [K]$, we have $\sum_{q=1}^M a_{k,q} = 1$ and $a_{k,q} \geq 0$ for all $q \in [M]$) and, additionally, we have

$$\sum_{k=1}^K a_{k,q} \frac{m_k}{m} = \frac{1}{M}, \quad \text{for all } q \in [M]. \quad (1)$$

The condition (1) ensures that all parallel channels are used equally often. The set of all valid bit mapper matrices is denoted by \mathcal{A} . As a baseline, we consider the “uniform” bit mapper \mathbf{A}_{uni} , where $a_{k,q} = 1/M$ for all $k \in [K]$ and $q \in [M]$.

The bit mapper matrix only determines the *fraction* of coded bits from a VN class that is allocated to a particular BEC. It does not determine which particular bit is sent through which channel. We assume that the actual allocation is determined uniformly at random, individually for each VN class. Such a random allocation effectively acts as though each VN class is subject to a (potentially) different erasure probability. In other words, one may think about transmitting the coded bits from different VN classes through different “virtual” BECs. The erasure probability for the k -th VN class is denoted by \tilde{p}_k and is given by

$$\tilde{p}_k = \sum_{q=1}^M a_{k,q} p_q. \quad (2)$$

As an example, for the baseline bit mapper, all virtual BECs have the same erasure probability $(\sum_{q=1}^M p_q)/M$.

IV. ASYMPTOTIC PERFORMANCE ANALYSIS

A. Iterative Bounded-Distance Decoding

We employ ℓ iterations of BDD for all component codes. In particular, each component code is assumed to correct all erasure patterns with weight up to its erasure-correcting capability. We are interested in characterizing the asymptotic performance of the overall iterative decoder as $n \rightarrow \infty$.

B. Erasure Probability Scaling

For any fixed set of erasure probabilities p_1, \dots, p_M , it can be shown that the decoding will fail with high probability as $n \rightarrow \infty$. This is a simple consequence of the assumed finite erasure-correcting capabilities of the component codes, while at the same time the expected number of erasures per component code grows without bounds.

In order to allow for a meaningful asymptotic analysis, we fix some positive constants c_1, \dots, c_M and then consider the case where $p_1 = c_1/n, \dots, p_M = c_M/n$. In other words, we assume that the erasure probability for each BEC decays slowly to zero as $n \rightarrow \infty$. Due to the vanishing erasure probabilities, it is tempting to conjecture that the decoding will now always be successful in the asymptotic limit. However, the answer depends crucially on the choice of c_1, \dots, c_M . Therefore, it is instructive to think about the constants c_1, \dots, c_M as *effective channel qualities*.

Due to the linearity of (2), the bit mapper converts the effective channel qualities for the parallel BECs into effective channel qualities for the virtual BECs denoted by $\tilde{c}_1, \dots, \tilde{c}_K$, i.e., we have $\tilde{p}_k = \tilde{c}_k/n$, where \tilde{c}_k is a weighted average

of c_1, \dots, c_M . In the following, it is more convenient to use a different indexing for the effective channel quality \tilde{c}_k associated with the k -th VN class. In particular, we use the alternative notation $\tilde{c}_{t,t'}(i,j)$ instead of \tilde{c}_k , where i, j, t, t' are the four parameters that identify the k -th VN class (see Section II-A).

C. Density Evolution

For the asymptotic DE analysis, one parameter is tracked per CN class as a function of the iteration number ℓ . The parameter is denoted by $x_{i,t}^{(\ell)}$ and its meaning is as follows. Consider a randomly chosen erased bit that is attached to a component code with class (i,t) . Then, the probability that this bit is *not* recovered after ℓ iterations by the component code converges asymptotically to $x_{i,t}^{(\ell)}$.

It can be rigorously shown that the parameter evolves as

$$x_{i,t}^{(\ell)} = \Psi_{\geq t} \left(\frac{1}{L} \sum_{j=1}^L \eta_{i,j} \sum_{t'=1}^{t_{\max}} \tilde{c}_{t,t'}(i,j) \tau_{t'}(j) x_{j,t'}^{(\ell-1)} \right), \quad (3)$$

where $\Psi_{\geq t}(x) \triangleq 1 - \sum_{i=0}^{t-1} \frac{x^i}{i!} e^{-x}$ is the tail probability of a Poisson random variable and, initially, we have $x_{i,t}^{(0)} = 1$ for all i and t . Due to space constraints, we only provide some intuition behind (3).¹ In particular, assume that we perform only one iteration, i.e., $\ell = 1$. Fix a randomly chosen erased bit attached to a class- (i,t) component code. The bit will not be recovered if t or more additional erasures are attached to the same component code. To compute the corresponding *probability* of not recovering the bit, it is therefore sufficient to characterize the distribution of the number of additional erasures. To do so, observe that the bits of a class- (i,t) component code are split up into different sections corresponding to different VN classes (see for example the dotted lines in Figs. 1(b) or 2(b), where sections are indicated by different colors). The number of bits per section is given by $\tau_{t'}(j)d$ and each bit in a given section is erased independently with probability $\tilde{c}_{t,t'}(i,j)/n$. As $n \rightarrow \infty$, the total number of erased bits per section thus converges to a Poisson random variable with mean $\tau_{t'}(j)d\tilde{c}_{t,t'}(i,j)/n = \tau_{t'}(j)\tilde{c}_{t,t'}(i,j)/L$. By considering all sections in a class- (i,t) component code (i.e., enumerating over all pairs (j,t')), we find that the total number of erasures is Poisson distributed with mean

$$\frac{1}{L} \sum_{j=1}^L \eta_{i,j} \sum_{t'=1}^{t_{\max}} \tilde{c}_{t,t'}(i,j) \tau_{t'}(j). \quad (4)$$

This gives (3) for $\ell = 1$. For subsequent iterations, we argue as follows. Assume that at the start of iteration ℓ , erased bits in section (j,t') have been recovered by class- (j,t') component codes independently with probability $1 - x_{j,t'}^{(\ell-1)}$. In this case, the distribution of the (remaining) additional erasures is still Poisson, albeit with a reduced mean parameter according to the term inside the brackets in (3).

¹The result is a straightforward generalization of [8, Th. 2]. Compared to the proof of [8, Th. 2], the only difference is to take into account the different erasure probabilities for different VN classes. However, this difference is easily captured in the inhomogeneous random graph model [14].

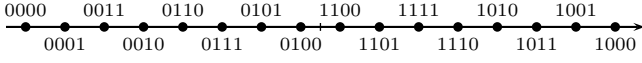


Fig. 3. 16-PAM labeled with the binary reflected Gray code.

D. Decoding Thresholds

The DE parameters in (3) depend on the code parameters, the bit mapper matrix, and the values of the effective channel qualities c_1, \dots, c_M . The latter dependence is made explicit by writing $x_{i,t}^{(\ell)}(c)$, where $c \triangleq (c_1, \dots, c_M)^T$. We say that a certain set of effective channel qualities is admissible if $\lim_{\ell \rightarrow \infty} x_{i,t}^{(\ell)}(c) = 0$ for all i and t . This corresponds to the case where decoding will be successful with high probability, provided that the code length and the number of decoding iterations are sufficiently large. Characterizing the set of all admissible effective channel qualities then leads to a threshold region (for a given code and bit mapper).

For some scenarios, including the coded modulation setup described in the next section, the effective channel qualities are parametrized by a single parameter $c > 0$. This allows us to define a one-dimensional decoding threshold. In particular, consider the following simple linear parametrization. Fix some constants $b_q > 0$ for $q \in [M]$ such that $(\sum_{q=1}^M b_q)/M = 1$. The effective channel qualities are then given by $c_q = cb_q$. The DE parameters now effectively only depend on c , i.e., the average effective channel quality, and we may write $x_{i,t}^{(\ell)}(c)$. The decoding threshold in this case is defined as

$$\bar{c} = \sup\{c > 0 \mid \lim_{\ell \rightarrow \infty} x_{i,t}^{(\ell)}(c) = 0 \text{ for all } i, t\}. \quad (5)$$

E. Parallel Binary Symmetric Channels

Typically, GPCs are used to correct errors and not erasures. Studying parallel BECs is merely a trick in order to allow for a rigorous asymptotic analysis. The problem with analyzing iterative BDD over BSCs is that the component code decoders may introduce undetected errors into the decoding process. This happens whenever the noise vector is such that it moves the transmitted codeword from the correct decoding sphere into a decoding sphere corresponding to another codeword. In that case, we say that the component code decoder miscorrects.

In terms of analysis, the prevailing approach in the literature (and also the one adopted here) is to assume that a genie prevents miscorrections. Under this assumption, the DE analysis in Section IV-C also applies to the transmission over a set of parallel BSCs, where all previously defined erasure probabilities are now interpreted as crossover probabilities. Furthermore, the erasure-correcting capabilities of the component codes are interpreted as error-correcting capabilities.

V. HIGHER-ORDER MODULATION

In this section, we describe how the asymptotic DE analysis in the previous section can be used to predict the code performance in a coded modulation scenario, in particular a BICM system with a hard-decision detector.

Consider the additive white Gaussian noise (AWGN) channel $Y = X + Z$, where Z is a zero-mean Gaussian random variable with variance $\sigma^2 = \mathbb{E}[Z^2]$. The operating point of

this channel is characterized by the signal-to-noise ratio (SNR) $\rho = \mathbb{E}[X^2]/\sigma^2$. We assume that the channel input X is constrained to a 2^M -PAM constellation $\mathcal{X} = \{\pm(2i-1) \mid i \in [2^{M-1}]\}$ which is labeled with the binary reflected Gray code. Fig. 3 shows the case where $M = 4$, i.e., 16-PAM. Constellation points are selected by mapping the coded bits (in batches of size M) to the labeling bits of the constellation. At the receiver, a minimum-distance symbol-by-symbol detector is used to output a hard decision on the labeling bits.

A useful (but not necessarily exact) abstraction of this setup is to imagine that the coded bits are transmitted over M parallel independent BSCs. For sufficiently high ρ , the nearest-neighbor approximation can be applied to characterize the crossover probability of the q -th BSC (corresponding to the q -th bit position of the labeling) as $p_q = b_q \bar{p}(\rho)$, where $b_q = M2^{q-1}/(2^M - 1)$ for $q \in [M]$,

$$\bar{p}(\rho) = \frac{2^M - 1}{M2^{M-1}} Q\left(\sqrt{\frac{3\rho}{2^{2M} - 1}}\right), \quad (6)$$

is the average crossover probability as a function of the SNR ρ , and $Q(\cdot)$ denotes the Q-function.

Assuming a sufficiently large (and finite) n , one can use the DE analysis in the previous section to predict the SNR region where the bit error rate (BER) performance curve of the code $\mathcal{C}_n(\eta, \tau)$ bends into the waterfall behavior. In particular, we can use the linear parameterization described in Section IV-D, where the constants b_q are as defined above. The DE analysis then gives a threshold in terms of the average effective channel quality c (see (5)), where we recall that the crossover probabilities are given by $p_q = cb_q/n$. Since we also have $p_q = b_q \bar{p}(\rho)$, we can convert any effective channel quality c for a fixed n into an SNR according to $\rho = \bar{p}^{-1}(c/n)$, where \bar{p}^{-1} is the inverse of (6). For example, for $M = 4$, $c = 10.63$, and $n = 1600$, we obtain $\rho = \bar{p}^{-1}(c/n) \approx 26.11$ dB.

It is, however, important to stress that the considered GPCs do not have decoding thresholds in terms of the SNR ρ . Rather, the studied scaling of the crossover probabilities corresponds to the limit $\rho \rightarrow \infty$. The calculated SNR values for finite n merely give an estimate about the SNR region where the waterfall region should be expected.

VI. BIT MAPPER OPTIMIZATION

As an application, we consider the problem of optimizing the bit mapper for a fixed GPC. For simplicity, we restrict ourselves to irregular HPCs where $L = 1$ and $\eta = 1$, i.e., the case where the Tanner graph consists of only a single position (see Example 2). The code array corresponds to the one shown in Fig. 2. To lighten the notation, position indices are dropped. In particular, the distribution specifying different error-correcting capabilities is denoted by $\tau = (\tau_1, \dots, \tau_{t_{\max}})$. For the optimization, we consider a distribution τ with two mass points according to $\tau_5 = 0.667$ and $\tau_8 = 0.333$. This gives rise to $K = 3$ different VN classes. The indexing of the VN classes is done according to $k(5, 5) = 1$, $k(5, 8) = 2$, $k(8, 8) = 3$, where the notation $k(t, t')$ indicates that the k -th VN class corresponds to bits that are protected by component

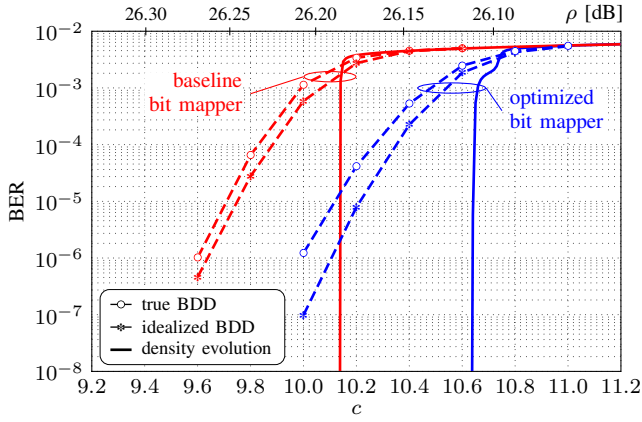


Fig. 4. Simulation results

codes with erasure-correcting capabilities t and t' . In the following, the signal constellation is assumed to be 16-PAM as shown in Fig. 3, i.e., we have $M = 4$ with $b_1 = 0.267$, $b_2 = 0.533$, $b_3 = 1.067$, and $b_4 = 2.133$.

In order to emphasize the dependence of the decoding threshold on the bit mapper matrix, we denote the threshold by $\bar{c}(\mathbf{A})$. For the given parameters, we obtain for example $\bar{c}(\mathbf{A}_{\text{uni}}) \approx 10.13$ assuming the baseline bit mapper. Our goal is to improve the threshold by choosing a different bit mapper. The corresponding optimization problem can be written as $\max_{\mathbf{A} \in \mathcal{A}} \bar{c}(\mathbf{A})$. One subtlety that arises for HPCs is that the ratio m_k/m in (1) depends on n , and hence also the set of valid bit mapper matrices \mathcal{A} . Therefore, we replace the “relative subblock size” m_k/m in (1) with the asymptotic version $\tilde{m}_k = \lim_{n \rightarrow \infty} m_k/m$, where \tilde{m}_k is either τ_t^2 or $2\tau_t\tau_{t'}$ for HPCs. We implemented a simple heuristic optimization solver based on the differential evolution algorithm [15] in order to obtain a (possibly suboptimal) solution to this optimization problem. The found optimized bit mapper matrix is

$$\mathbf{A}^* = \begin{pmatrix} 0.2640 & 0.1056 & 0.2984 & 0.3320 \\ 0.2976 & 0.4508 & 0.2453 & 0.0063 \\ 0.0031 & 0.0249 & 0.0746 & 0.8973 \end{pmatrix}, \quad (7)$$

with an improved threshold of $\bar{c}(\mathbf{A}^*) \approx 10.63$. The solution is not necessarily globally optimal, due to the heuristic nature of the solver. From the optimized bit mapper matrix, one can see for example that bits from the 3rd VN class with the highest protection level (i.e., the last row in \mathbf{A}^*) are allocated mainly to the labeling bit which is least reliable.

We simulated the code $\mathcal{C}_n(\boldsymbol{\eta}, \boldsymbol{\tau})$ for $n = 1600$ with the baseline and optimized bit mappers² over the AWGN channel with $\ell = 50$ iterations of BDD. For the chosen parameters, some rounding is required in the sense that we use $\lfloor n\tau_5 \rfloor = 1067$ and $\lceil \tau_8 n \rceil = 533$ component codes with the two different erasure-correcting capabilities. Note that the code has length $m = 1,279,200$ (where $m_1 = m_2 = 568,711$ and $m_3 = 141,778$), which is considered acceptable for fiber-optical communications due to the high data rates. Furthermore, assuming binary primitive BCH codes as component

codes, it can be shown that the code rate is lower-bounded by $R \geq 0.92$, see [8, Sec. VII-D]. Fig. 4 shows the simulation results by the dashed lines, where dots correspond to true BDD and stars to idealized BDD with no miscorrections. The DE prediction is shown by the solid lines and accurately predicts the waterfall regions of the two systems. By using the optimized bit mapper, one obtains a modest improvement of ≈ 0.06 dB at a BER of 10^{-6} . This improvement is, however, obtained virtually “for free”, i.e., it entails only a reallocation of the coded bits to the signal constellation.

VII. CONCLUSIONS AND FUTURE WORK

In this paper, we characterized the asymptotic performance of deterministic GPCs over parallel BECs assuming iterative BDD. It was shown that the analysis accurately predicts the code performance in a BICM system with a hard-decision detector. We used the analysis to optimize the bit mapper, which leads to moderate performance improvements at almost no increased system complexity (e.g., some additional buffering may be required). For future work, it could be interesting to study the joint design of the code and bit mapper.

REFERENCES

- [1] P. Elias, “Error-free coding,” *IRE Trans. Inf. Theory*, vol. 4, no. 4, pp. 29–37, Apr. 1954.
- [2] J. Justesen, K. J. Larsen, and L. A. Pedersen, “Error correcting coding for OTN,” *IEEE Commun. Mag.*, vol. 59, no. 9, pp. 70–75, Sep. 2010.
- [3] “Forward error correction for high bit-rate DWDM submarine systems,” ITU-T Recommendation G.975.1, 2004.
- [4] B. P. Smith, A. Farhood, A. Hunt, F. R. Kschischang, and J. Lodge, “Staircase codes: FEC for 100 Gb/s OTN,” *J. Lightw. Technol.*, vol. 30, no. 1, pp. 110–117, Jan. 2012.
- [5] Y.-Y. Jian, H. D. Pfister, K. R. Narayanan, R. Rao, and R. Mazahreh, “Iterative hard-decision decoding of braided BCH codes for high-speed optical communication,” in *Proc. IEEE Glob. Communication Conf. (GLOBECOM)*, Atlanta, GA, 2014.
- [6] L. Beygi, E. Agrell, J. M. Kahn, and M. Karlsson, “Coded modulation for fiber-optic networks,” *IEEE Signal Processing Mag.*, vol. 31, no. 2, pp. 93–103, Mar. 2014.
- [7] B. Smith and F. R. Kschischang, “A pragmatic coded modulation scheme for high-spectral-efficiency fiber-optic communications,” *J. Lightw. Technol.*, vol. 30, no. 13, pp. 2047–2053, Jul. 2012.
- [8] C. Häger, H. D. Pfister, A. Graell i Amat, and F. Brännström, “Density evolution for deterministic generalized product codes on the binary erasure channel,” *submitted to IEEE Trans. Inf. Theory*, 2015. [Online]. Available: <http://arxiv.org/pdf/1512.00433.pdf>
- [9] C. Häger, A. Graell i Amat, F. Brännström, A. Alvarado, and E. Agrell, “Improving soft FEC performance for higher-order modulations via optimized bit channel mappings,” *Opt. Express*, vol. 22, no. 12, pp. 14 544–14 558, Jun. 2014.
- [10] R. Tanner, “A recursive approach to low complexity codes,” *IEEE Trans. Inf. Theory*, vol. 27, no. 5, pp. 533–547, Sep. 1981.
- [11] J. Justesen, “Performance of product codes and related structures with iterated decoding,” *IEEE Trans. Commun.*, vol. 59, no. 2, pp. 407–415, Feb. 2011.
- [12] H. D. Pfister, S. K. Emmadi, and K. Narayanan, “Symmetric product codes,” in *Proc. Information Theory and Applications Workshop (ITA)*, San Diego, CA, 2015.
- [13] C. Häger, H. D. Pfister, A. Graell i Amat, and F. Brännström, “Density evolution and error floor analysis of staircase and braided codes,” in *Proc. Optical Fiber Communication Conf. (OFC)*, Anaheim, CA, 2016.
- [14] B. Bollobás, S. Janson, and O. Riordan, “The phase transition in inhomogeneous random graphs,” *Random Structures and Algorithms*, vol. 31, no. 1, pp. 3–122, Aug. 2007.
- [15] R. Storn and K. Price, “Differential evolution—a simple and efficient heuristic for global optimization over continuous spaces,” *J. Global Opt.*, vol. 11, pp. 341–359, Nov. 1997.

²To determine the actual number of bits to be allocated for finite values of n , appropriate modifications (e.g., rounding) of the matrix $m\mathbf{A}^*$ are required.